

# M<sup>3</sup>-VRD: Multimodal Multi-task Multi-teacher Visually-Rich Form Document Understanding

Anonymous ACL submission

## Abstract

This paper presents a groundbreaking multimodal, multi-task, multi-teacher joint-grained knowledge distillation model for visually-rich form document understanding. The model is designed to leverage insights from both fine-grained and coarse-grained levels by facilitating a nuanced correlation between token and entity representations, addressing the complexities inherent in form documents. Additionally, we introduce new inter-grained and cross-grained loss functions to further refine diverse multi-teacher knowledge distillation transfer process, presenting distribution gaps and a harmonised understanding of form documents. Through a comprehensive evaluation across publicly available form document understanding datasets, our proposed model consistently outperforms existing baselines, showcasing its efficacy in handling the intricate structures and content of visually complex form documents.

## 1 Introduction

Understanding and extracting structural information from Visually-Rich Documents (VRDs), such as academic papers (Zhong et al., 2019; Ding et al., 2023b), receipts (Park et al., 2019), and forms (Jaume et al., 2019; Ding et al., 2023a), holds immense value for Natural Language Processing (NLP) tasks, particularly in information extraction and retrieval. While significant progress has been made in solving various VRD benchmark challenges, including layout analysis and table structure recognition, the task of form document understanding remains notably challenging. This complexity of the form document understanding arises from two main factors: 1) the involvement of two distinct authors in a form and 2) the integration of diverse visual cues. Firstly, forms mainly involve two primary authors: form designers and users. Form designers create a structured form to collect necessary information as a user interface. Unfortunately, the form layouts, designed to collect varied

information, often lead to complex logical relationships, causing confusion for form users and heightening the challenges in form document understanding. Secondly, diverse authors in forms may encounter a combination of different document natures, such as digital, printed, or handwritten forms. Users may submit forms in various formats, introducing noise such as low resolution, uneven scanning, and unclear handwriting. Traditional document understanding models do not account for the diverse carriers of document versions and their associated noises, exacerbating challenges in understanding form structures and their components. Most VRD understanding models inherently hold implicit multimodal document structure analysis (Vision and Text understanding) knowledge either at fine-grained (Huang et al., 2022; Wang et al., 2022) or coarse-grained (Tan and Bansal, 2019; Li et al., 2019) levels. The fine-grained only models mainly focus on learning detailed logical layout arrangement, which cannot handle complex relationships of multimodal components, while the coarse-grained models tend to omit significant words or phrases. Hence, we introduce a novel joint-grained document understanding approach with multimodal multi-teacher knowledge distillation. This method leverages knowledge from various task-based teachers (pre-trained models) throughout the training process, intending to create more inclusive and representative multi- and joint-grained document representations.

Our contributions can be summarised as follows: 1) We present a groundbreaking multimodal, multi-task, multi-teacher joint-grained knowledge distillation model designed explicitly to understand visually-rich form documents. 2) The proposed model outperforms across publicly available form document datasets. 3) To the best of our knowledge, this research marks the first in adopting multi-task knowledge distillation, focusing on incorporating multimodal form document components.

Model	Modalities	Pre-training Datasets	Pre-training Tasks	Downstream Tasks	Granularity
Donut (2022)	V	IIT-CDIP	NTP	DC, VQA, KIE	Token
Pix2struct (2023b)	V	C4 corpus	NTP	VQA	Token
LiLT (2022)	T, S	IIT-CDIP	MVLM, KPL, CAI	DC, KIE	Token
BROS (2022)	T, S	IIT-CDIP	MLM, A-MLM	KIE	Token
LayoutLMv3 (2022)	T, S, V	IIT-CDIP	MLM, MIM, WPA	DC, VQA, KIE	Token
DocFormerv2 (2023)	T, S, V	IDL	TTL, TTG, MLM	DC, VQA, KIE	Token
Fast-StrucText (2023)	T, S, V	IIT-CDIP	MVLM, GTR, SOP, TIA	KIE	Token
FormNetV2 (2023a)	T, S, V	IIT-CDIP	MLM, GCL	KIE	Token
M <sup>3</sup> -DVQA (Ours)	T, S, V	FUNSD, FormNLU	Multi-teacher Knowledge Distillation	KIE	Token, Entity

Table 1: Comparison with state-of-the-art models for receipt and form understanding. In the *Modalities* column, *T* represents Textual information, *V* represents Visual information, and *S* represents Spatial information.

## 2 Related Works

Visually Rich Document (VRD) understanding entails comprehending the structure and content of documents by capturing the underlying relations between textual and visual modalities. Several downstream tasks such as Key Information Extraction (KIE), Document Classification (DC), and Visual Question Answering (VQA), have contributed to raise the attention of the multimodal learning community. In this work, we cope with form documents, whose structure and content are particularly challenging to understand (Srivastava et al., 2020). Form documents possess intricate structures, involving collaboration between form designers, who craft clear structures for data collection, and form users, who interact with the forms based on their comprehension, with clarity and ease of understanding being variable. Table 1 enumerates the main characteristics of the latest models proposed for document understanding.

**Vision-only approaches:** They exclusively rely on the visual representation (denoted by *V* modality in Table 1) of the document components thus circumventing the limitations of state-of-the-art text recognition tools (e.g., Donut (Kim et al., 2022) and Pix2struct (Lee et al., 2023b)). Their document representations are commonly pre-trained using a Next Token Prediction (NTP) strategy, offering alternative solutions to traditional techniques based on Natural Language Processing.

**Multimodal approaches:** They leverage both the recognised text and the spatial relations (denoted by *T* and *S*) between document components (see, for instance, LiLT (Wang et al., 2022) and BROS (Hong et al., 2022)). The main goal is to complement raw content understanding with layout information. Expanding upon this multimodal

framework, models such as LayoutLMv3 (Huang et al., 2022), DocFormerv2 (Appalaraju et al., 2023), Fast-StrucText (Zhai et al., 2023), and FormNetV2 (Lee et al., 2023a) integrate the visual modality with text and layout information. These approaches are capable of capturing nuances in the document content hidden in prior works. To leverage multimodal relations, these models are typically pre-trained in a multi-task fashion, exploiting a curated set of token- or word-based pre-training tasks, such as masking or alignment.

**Our approach** aligns with the multimodal model paradigm, distinguishing itself by eschewing generic pre-training tasks reliant on masking, alignment, or NTP. Instead, it leverages the direct extraction of knowledge from *multiple teachers*, each trained on downstream datasets, encompassing *both entity and token levels* of analysis with the proposed inter-grained and cross-grained losses. This enriches the depth of understanding in visual documents, capturing intricate relationships and semantic structures beyond individual tokens.

## 3 Methodology

As previously noted, our paper focuses on interpreting visually rich documents, particularly form documents created and used collaboratively by multiple parties. To accomplish this objective, we introduce and employ two tiers of multimodal information: fine-grained and coarse-grained levels, which play a crucial role in understanding the structure and content of an input form page. Note that existing pre-trained visual-language models, whether designed for generic documents, possess implicit knowledge on either fine-grained or coarse-grained aspects. Hence, we propose an approach that harnesses knowledge from diverse pre-trained models throughout training. This strategy aims to generate

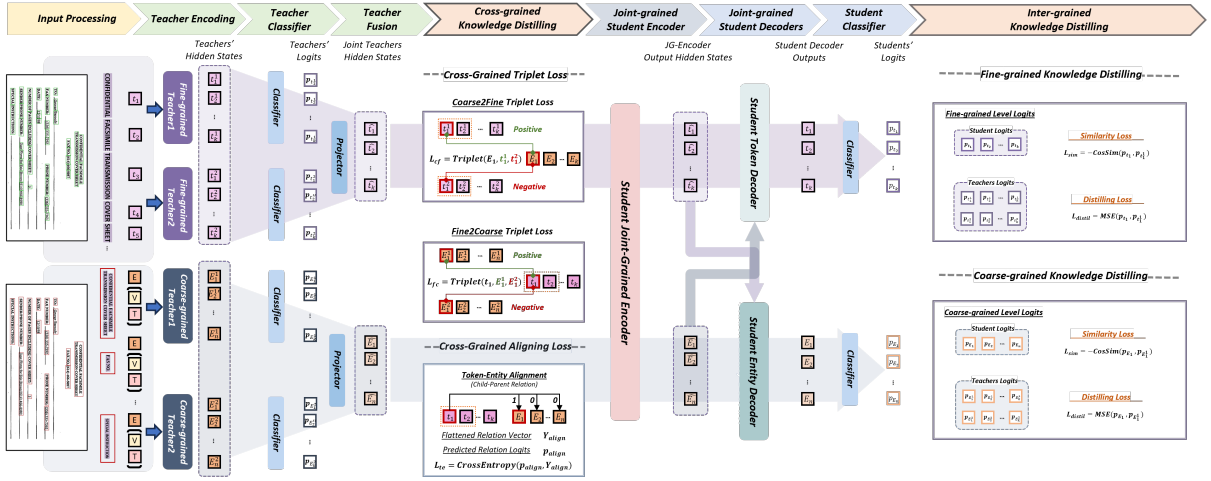


Figure 1: Multimodal Multi-task Multi-Teacher Joint-Grained Document Understanding Framework. Each section is aligned with the specific colours, Green: Section 3.2.1, Blue: Section 3.2.2, Orange: Section 3.3

157 more comprehensive and representative multi- and  
 158 joint-grained document representations, ultimately  
 159 enhancing the effectiveness of downstream tasks  
 160 related to document understanding.

### 161 3.1 Preliminary Definitions

162 Prior to going through our proposed approach in  
 163 detail, we would provide formal definitions for the  
 164 terminology employed throughout this paper. We  
 165 believe establishing clear and precise definitions  
 166 could contribute to a comprehensive understanding  
 167 of the concepts and terms integral to our research.

168 **1) Fine-grained Document Understanding**  
 169 (Huang et al., 2022; Wang et al., 2022; Hong  
 170 et al., 2022) is a pivotal aspect of document  
 171 analysis, involving frameworks that offer de-  
 172 tailed insights to comprehend document content,  
 173 particularly when addressing token-level tasks,  
 174 such as span-based information extraction and  
 175 question answering. Regarding *input features*,  
 176 existing pre-trained models at the fine-grained level  
 177 harness multimodal features, such as positional  
 178 information and image-patch embedding, to en-  
 179 hance the fine-grained token representations. The  
 180 *pre-training phase* incorporates several learning  
 181 techniques, including Masked Visual-Language  
 182 Modelling, Text-Image Matching, and Multi-label  
 183 Document Classification, strategically designed to  
 184 acquire inter or cross-modality correlations and  
 185 contextual knowledge. However, it is essential  
 186 to acknowledge the *limitations* of fine-grained  
 187 frameworks, as their primary focus lies in learning  
 188 the logical and layout arrangement of input  
 189 documents. These frameworks may encounter

190 challenges in handling complex multimodal  
 191 components.

192 **2) Coarse-grained Document Understanding**  
 193 (Tan and Bansal, 2019; Li et al., 2019) is a  
 194 vital component in document analysis, with frame-  
 195 works adept at grasping the logical relations and  
 196 layout structures within input documents. Particu-  
 197 larly well-suited for tasks like document compo-  
 198 nent entity parsing, coarse-grained models excel  
 199 in capturing high-level document understanding.  
 200 Despite the dominant trend of fine-grained docu-  
 201 ment understanding models, some research recog-  
 202 nises (Tan and Bansal, 2019; Li et al., 2019) that  
 203 the knowledge from general domain-based Visual-  
 204 Language Pre-trained Models (VLPMS) could be  
 205 leveraged to form a foundational document under-  
 206 standing. However, the coarse-grained document  
 207 understanding models have significant *limitations*,  
 208 including their tendency to overlook detailed in-  
 209 formation, leading to the omission of significant  
 210 words or phrases. Preliminary entity-level anno-  
 211 tations are often necessary, and the current back-  
 212 bone models are pre-trained on the general domain,  
 213 highlighting the need for document domain frame-  
 214 works specifically pre-trained at the coarse-grained level.

### 215 3.2 Multimodal Multi-task Multi-teacher 216 Joint-grained Document Understanding<sup>1</sup>

217 Therefore, we introduce a joint-grained document  
 218 understanding framework  $\mathcal{F}_{jg}$ , designed to harness  
 219 pre-trained knowledge from both fine-grained and  
 220 coarse-grained levels. Our approach integrates in-

<sup>1</sup>Subsections are aligned with different colour in Figure 1, Green: Section 3.2.1, Blue: Section 3.2.2, Orange: Section 3.3

sights from multiple pre-trained backbones, facilitating a unified understanding of document content encompassing detailed nuances and high-level structures. It aims to synergise the strengths of fine-grained and coarse-grained models, enhancing the overall effectiveness of form understanding tasks.

### 3.2.1 Multimodal Multi-task Multi-Teacher

To facilitate this joint-grained framework, we employ **Multimodal Multi-teachers** from two **Multi-tasks**, fine-grained and coarse-grained tasks within our framework. While the fine-grained teacher  $\mathcal{F}_{fg}$  is characterised by checkpoints explicitly fine-tuned for the **token classification**, the coarse-grained teacher  $\mathcal{F}_{cg}$  utilises fine-tuning checkpoints for the document component **entity classification**. The details of fine-grained and coarse-grained teacher models are articulated in Section 4.3. The ablation study of those teacher models is in Section 5.2.  $\mathcal{F}_{fg}$  and  $\mathcal{F}_{cg}$  get the encoded inputs of token and entity level, respectively, to acquire the corresponding last layer hidden states and logits for downstreaming procedures. For example, after feeding the sequence of tokens  $\tilde{\mathbf{t}} = \{\tilde{t}_1, \tilde{t}_2, \dots, \tilde{t}_k\}$  and sequence of multimodal entity embeddings  $\tilde{\mathbf{E}} = \{\tilde{E}_1, \tilde{E}_2, \dots, \tilde{E}_n\}$  into  $\mathcal{F}_{fg1}$  and  $\mathcal{F}_{cg1}$ , respectively, we acquire the hidden states  $\mathbf{t}^1 = \{t_1^1, t_2^1, \dots, t_k^1\}$  and  $\mathbf{E}^1 = \{E_1^1, E_2^1, \dots, E_n^1\}$ , as well as classification logits  $\mathbf{p}_{t^1} = \{p_{t_1^1}, p_{t_2^1}, \dots, p_{t_k^1}\}$  and  $\mathbf{p}_{\mathbf{E}^1} = \{p_{E_1^1}, p_{E_2^1}, \dots, p_{E_n^1}\}$ . Supposing  $\mathbb{T} = \{\mathbf{t}^1, \mathbf{t}^2, \dots\}$  and  $\mathbb{E} = \{\mathbf{E}^1, \mathbf{E}^2, \dots\}$  are hidden states from multiple teachers, the combined representations are fed into corresponding projection layers  $\mathcal{L}_{fg}$  and  $\mathcal{L}_{cg}$  to get the multi-teacher representations  $\hat{\mathbf{t}} = \{\hat{t}_1, \hat{t}_2, \dots, \hat{t}_k\}$  and  $\hat{\mathbf{E}} = \{\hat{E}_1, \hat{E}_2, \dots, \hat{E}_n\}$  for each grain.

### 3.2.2 Joint-Grained Learning

Our joint-grained learning framework comprises Joint-grained Encoder and Decoders.

**The joint-grained encoder**  $\mathcal{E}$ , implemented as a transformer encoder, is designed to learn the contextual correlation between fine-grained  $\hat{\mathbf{t}}$  and coarse-grained  $\hat{\mathbf{E}}$  representations. This enables the model to capture nuanced details at the token level while simultaneously grasping the high-level structures represented by entities within the document. **The joint-grained decoders**  $\mathcal{D}$  play a crucial role in processing the augmented joint-grained representations. For the fine-grained decoder  $\mathcal{D}_{fg}$ , the input comprises fine-grained token representations  $\hat{\mathbf{t}}$ , with the entity representation serving as memory  $\hat{\mathbf{E}}$ .

This configuration allows the decoder to focus on refining and generating augmented token representations  $\mathbf{t}$  based on the contextual information provided by both token and entity representations. In contrast, for coarse-grained decoder  $\mathcal{D}_{cg}$ , the input is the entity representation  $\hat{\mathbf{E}}$ , while the memory consists of token representations  $\hat{\mathbf{t}}$ . This approach enables the coarse-grained decoders to emphasise broader structures and relationships at the entity level, leveraging the memory of fine-grained token information to generate a more comprehensive entity representation  $\mathbf{E}$ . Overall, the proposed joint-grained architecture facilitates a comprehensive understanding of document content by incorporating fine-grained and coarse-grained perspectives.

The pre-training of different teacher models involves diverse techniques and features, so a simplistic approach of merely concatenating or pooling hidden states may not fully leverage the individual strengths of each model. Traditional self-/cross attention-based transformer encoders or decoders might encounter challenges in integrating knowledge from various grains, potentially introducing noise to specific grained weights. To address this concern, we propose using multiple types of losses to thoroughly explore implicit knowledge within the diverse teachers (pre-trained models).

### 3.3 Multimodal Multi-task Multi-Teacher Knowledge Distillation

This section introduces the multi-loss strategy to enhance inter-grained and cross-grained knowledge exchange, ensuring a more nuanced and effective integration of insights from fine-grained and coarse-grained representations. The accompanying multi-loss ablation study (Section 5.3) aims to optimise the synergies between multiple teacher models, thereby contributing to a more robust and comprehensive joint-grained learning process.

#### 3.3.1 Task-oriented Cross Entropy Loss

The Task-oriented Cross Entropy (CE) loss is pivotal in facilitating a task-based knowledge distillation strategy. This is computed by comparing the predictions of the student model with the ground truth for each specific task. Adopting the CE loss provides the student model with direct supervisory signals, thereby aiding and guiding its learning process. Note that we address two task-oriented CE losses within our proposed approach, one from the token classification task and the other from the entity classification task. The output hidden

states from  $\mathcal{D}_{fg}$  and  $\mathcal{D}_{cg}$  are fed into classifiers to get the output logits  $\mathbf{p}_t = \{p_{t_1}, p_{t_2}, \dots, p_{t_k}\}$  and  $\mathbf{p}_E = \{p_{E_1}, p_{E_2}, \dots, p_{E_n}\}$ . Supposing the label sets for fine-grained and entity-level tasks are  $\mathbf{Y}_t = \{y_{t_1}, y_{t_2}, \dots, y_{t_k}\}$  and  $\mathbf{Y}_E = \{y_{E_1}, y_{E_2}, \dots, y_{E_n}\}$ , the fine-grained and coarse-grained Task-oriented Cross Entropy losses  $l_t$  and  $l_E$  are calculated as:

$$l_t = CrossEntropy(\mathbf{p}_t, \mathbf{Y}_t) \quad (1)$$

$$l_e = CrossEntropy(\mathbf{p}_E, \mathbf{Y}_E) \quad (2)$$

### 3.3.2 Inter-Grained Loss Functions

Since various pre-trained models provide different specific knowledge to understand the form comprehensively, effectively distilling valuable information from selected fine-tuned checkpoints may generate more representative token representations. In addressing this, we introduce two target-oriented loss functions tailored to distil knowledge from teachers at different levels. These aim to project the label-based distribution from fine-grained  $\mathbf{p}_T = \{\mathbf{p}_{t^1}, \mathbf{p}_{t^2}, \dots\}$  or coarse-grained teacher logits  $\mathbf{p}_E = \{\mathbf{p}_{E^1}, \mathbf{p}_{E^2}, \dots\}$  to corresponding student logits  $\mathbf{p}_t$  and  $\mathbf{p}_E$ , enabling efficient learning of label distributions.

**Similarity Loss:** This is introduced as an effective method to distil knowledge from the output logits  $\mathbf{p}_t$  and  $\mathbf{p}_E$  of selected fine-grained or coarse-grained teacher checkpoints from  $\mathbf{p}_T$  and  $\mathbf{p}_E$ . It aims to mitigate the logit differences between the student classifier and the chosen teachers using cosine similarity (*CosSim*), promoting a more aligned understanding of the label-based distribution. Supposing we have  $n_t$  and  $n_e$  teachers for fine-grained and coarse-grained tasks, respectively, the similarity loss of fine-grained  $l_{sim_t}$  and coarse-grained  $l_{sim_e}$  can be calculated by:

$$l_{sim_t} = - \sum_i^{i=n_t} \sum_j^{j=k} CosSim(p_{t_j^i}, p_{t_j}) \quad (3)$$

$$l_{sim_e} = - \sum_i^{i=n_e} \sum_j^{j=n} CosSim(p_{E_j^i}, p_{E_j}) \quad (4)$$

**Distilling Loss:** Inspired by (Phuong and Lample, 2019), we adopt an extreme logit learning model for the distilling loss. This loss implements knowledge distillation using Mean Squared Error (*MSE*) between the students' logits  $\mathbf{p}_t$  and  $\mathbf{p}_E$  and the teachers' logit sets  $\mathbf{p}_T$  and  $\mathbf{p}_E$ . This method is employed to refine the knowledge transfer process further, promoting a more accurate alignment

between the student and teacher models.

$$l_{distil_t} = \frac{1}{k} \sum_j^{j=k} MSE(p_{t_j^i}, p_{t_j}) \quad (5)$$

$$l_{distil_e} = \frac{1}{n} \sum_j^{j=n} MSE(p_{E_j^i}, p_{E_j}) \quad (6)$$

The introduction of these inter-grained loss functions, including the similarity loss and the distilling loss, contributes to mitigating distribution gaps and fostering a synchronised understanding of the form across various levels of granularity.

### 3.3.3 Cross-Grained Loss Functions

In addition, we incorporate cross-grained loss functions. While fine-grained and coarse-grained information inherently align, the joint-grained framework employs self-attention and cross-attention to approximate the correlation between token and entity representations.  $\mathbb{T}$  and  $\mathbb{E}$  are teachers hidden states sets, each  $\mathbf{t}^i \in \mathbb{T}$  and  $\mathbf{E}^i \in \mathbb{E}$  are represented  $\mathbf{t}^i = \{t_1^i, t_2^i, \dots, t_k^i\}$  and  $\mathbf{E}^i = \{E_1^i, E_2^i, \dots, E_n^i\}$  and  $\mathbf{t}$  and  $\mathbf{E}$  are hidden states from student decoder.

**Cross-grained Triplet Loss:** Inherent in each grain feature are parent-child relations between tokens and aligned semantic form entities. The introduction of triplet loss aids the framework in automatically selecting more representative feature representations by measuring the feature distance from one grain to another-grained aligned representation. This effectively enhances joint-grained knowledge transfer, optimising the overall understanding of the form. For acquiring the loss  $l_{triplet_{fg}}$  to select fine-grained teachers based on coarse-grained distribution adaptively, we define the anchor as each entity  $E_i \in \mathbb{E}$  which has the paired token representations  $t_i^1 \in \mathbf{t}^1$  and  $t_i^2 \in \mathbf{t}^2$  (if the number of teachers is more significant than 2, randomly select two of them). The L-2 norm distance is used to measure the distance between fine-grained teachers ( $t_i^1, t_i^2$ ) and anchor  $E_j$ , where the more similar entities are treated as positive samples ( $t_i^{pos}$ ) otherwise negative ( $t_i^{neg}$ ). For coarse-grained triplet loss  $l_{triplet_{cg}}$ , the same measurements are adopted for coarse-grained teacher positive ( $E_j^{pos}$ ) and negative selection ( $E_j^{neg}$ ) for an anchor  $t_i$ . Supposing the  $j$ -th,  $l_{triplet_{fg}}$  and  $l_{triplet_{cg}}$  are defined:

$$l_{triplet_{fg}} = \frac{1}{k} \sum_i^{i=k} Triplets(E_j, t_i^{pos}, t_i^{neg}) \quad (7)$$

$$l_{triplet_{cg}} = \frac{1}{k} \sum_i^{i=k} Triplets(t_i, E_j^{pos}, E_j^{neg}) \quad (8)$$

414 As one entity is typically paired with more than one  
415 token, when calculating  $l_{triplet_{cg}}$ , we will consider  
416 all  $k$  entity-token pairs.

417 **Cross-grained Alignment Loss:** In addition to the  
418 triplet loss, designed to filter out less representative  
419 teachers, we introduce another auxiliary task. This  
420 task focuses on predicting the relations between  
421 tokens and entities, providing an additional layer  
422 of refinement to the joint-grained framework. The  
423 cross-grained alignment loss further contributes to  
424 the comprehensive learning and alignment of token  
425 and entity representations, reinforcing the joint-  
426 grained understanding of the form document. For  
427 an input form document page containing  $k$  tokens  
428 and  $n$  entities, we have a targeting tensor  $\mathbf{Y}_{align}$   
429 where  $Dim(\mathbf{Y}_{align}) = \mathbb{R}^{k \times n}$ . We use acquired  
430 alignment logit  $\mathbf{p}_{align} = \mathbf{t} \times \mathbf{E}$  to represent the pre-  
431 dicted token-entity alignments. The cross-grained  
432 alignment loss  $l_{align}$  can be calculated by:

$$433 \quad l_{align} = CrossEntropy(\mathbf{p}_{align}, \mathbf{Y}_{align}) \quad (9)$$

## 434 4 Evaluation Setup

### 435 4.1 Datasets<sup>2</sup>

436 **FUNSD** (Jaume et al., 2019) comprises 199 noisy  
437 scanned documents from various domains includ-  
438 ing marketing, advertising, and science reports, re-  
439 lated to US tobacco firms. It is split into train and  
440 test sets (149/50 documents), and each document  
441 is presented in either printed or handwritten format  
442 with low resolutions. Our evaluation focuses on  
443 the semantic-entity labeling task that identifies four  
444 predefined labels (i.e., question, answer, header,  
445 and other) based on input text content.

446 **FormNLU** (Ding et al., 2023a) consists of 867 fi-  
447 nancial form documents collected from Australian  
448 Stock Exchange (ASX) filings. It includes three  
449 form types: digital ( $D$ ), printed ( $P$ ), and handwrit-  
450 ten ( $H$ ), and is split into five sets: train- $D$  (535),  
451 val- $D$  (76), test- $D$  (146), test- $P$  (50), and test- $H$  (50  
452 documents) and supports two tasks: Layout Analy-  
453 sis and Key Information Extraction. Our evaluation  
454 focuses on the layout analysis that identifies seven  
455 labels (i.e., title, section, form key, form value, ta-  
456 ble key, table value, and others), detecting each  
457 document entity, especially for  $P$  and  $H$ , the com-  
458 plex multimodal form document.

### 459 4.2 Baselines and Metrics

460 For **token-level information extraction** baselines,  
461 we use three Document Understanding (DU) mod-

<sup>2</sup>The statistics of token/entity are shown in Table 5 and 6.

462 els: LayoutLMV3 (Huang et al., 2022), LiLT  
463 (Wang et al., 2022), and BROS (Hong et al., 2022).  
464 LayoutLMV3 employs a word-image patch align-  
465 ment, that utilises a document image along with  
466 its corresponding text and layout position infor-  
467 mation. In contrast, LiLT and BROS focus only  
468 on text and layout information without incorporat-  
469 ing images. LiLT uses a bi-directional attention  
470 mechanism across token embedding and layout  
471 embedding, whereas BROS uses a relative spatial  
472 encoding between text blocks. For **entity-level in-  
473 formation extraction** baselines, we use two vision-  
474 language (VL) models: LXMERT (Tan and Bansal,  
475 2019) and VisualBERT (Li et al., 2019). Com-  
476 pared to the two DU models, these VL models use  
477 both image and text input without layout informa-  
478 tion. LXMERT focuses on cross-modality learn-  
479 ing between word-level sentence embeddings and  
480 object-level image embeddings, while VisualBERT  
481 simply inputs image regions and text, relying on  
482 implicit alignments within the network. For **eval-  
483 uation metrics**, inspired by (Jaume et al., 2019)  
484 and (Ding et al., 2023a), we primarily use F1-score  
485 to represent both overall and detailed performance  
486 breakdowns, aligning with other baselines.

### 487 4.3 Implementation Details<sup>3</sup>

488 In token-level experiments, we fine-tuned  
489 LayoutLMV3-base using its text tokeniser  
490 and image feature extractor. We also fine-  
491 tuned LiLT combined with RoBERTa base. In  
492 entity-level experiments, we employ pre-trained  
493 BERT (748-d) for encoding textual content,  
494 while ResNet101(2048-d) is used for region-  
495 of-interest(RoI) feature to capture the visual  
496 aspect. These extracted features serve as input  
497 for fine-tuning LXMERT and VisualBERT. All  
498 fine-tuned models serve as teacher models. Our  
499 hyperparameter testing involves a maximum of 50  
500 epochs with learning rates set at 1e-5 and 2e-5. All  
501 are conducted on a Tesla V100-SXM2 with 16GB  
502 graphic memory and 51 GB memory, CUDA 11.2.

## 503 5 Results

### 504 5.1 Overall Performance

505 Extensive experiments are conducted to highlight  
506 the effectiveness of the proposed **Multimodal  
507 Multi-task Multi-Teacher** framework, including  
508 *joint-grained learning*, *multi-teacher* and *multi-  
509 loss* architecture. Table 2 shows representative

<sup>3</sup>Additional Implemntation Details are in Appendix D

Model	Config & Loss	FUNSD	FormNLU	
			<i>P</i>	<i>H</i>
BROS	Single Teacher	82.44	92.45	93.68
LiLT	Single Teacher	87.54	<u>96.50</u>	91.35
LayoutLMv3	Single Teacher	<u>90.61</u>	95.99	<u>97.39</u>
JG- $\mathcal{E}$	Joint Cross Entropy	90.45	94.91	96.55
JG- $\mathcal{D}$	Joint Cross Entropy	90.48	95.68	97.62
JG- $\mathcal{E}\&\mathcal{D}$	Joint Cross Entropy	90.57	95.93	97.62
MT-JG- $\mathcal{E}\&\mathcal{D}$ (Ours)	Joint Cross Entropy	90.53	97.21	97.75
	+ <i>Sim</i>	<b>91.05</b>	98.25	98.09
	+ <i>Distil</i>	90.90	98.12	97.72
	+ <i>Triplet</i>	90.28	97.58	97.28
	+ <i>Align</i>	90.55	97.24	97.42
	+ <i>Sim + Distil</i> + <i>Triplet + Align</i>	90.92	<b>98.69</b>	<b>98.39</b>

Table 2: Overall Performance of Model and Configurations on FormNLU printed *P* and handwritten *H*. The full form of acronyms can be found in Section 5.1. The best is in **bold**. The second best is underlined.

model configurations on various adopted modules. LayoutLMv3 performs notably superior to BROS and LiLT, except for the FormNLU printed test set. LayoutLMv3 outperforms around 3% and 4% the second-best baseline on FUNSD and FormNLU handwritten sets, respectively. This superiority can be attributed to LayoutLMv3’s utilisation of patched visual cues and textual and layout features, resulting in more comprehensive multimodal representations. So we found LayoutLMv3 would be a robust choice for fine-grained baselines in further testing<sup>4</sup>. To find the most suitable **Joint-Grained learning** (JG), we compare the results of single-teacher joint-grained frameworks including Encoder ( $\mathcal{E}$ ) only, Decoder ( $\mathcal{D}$ ) only, and Encoder with Decoder ( $\mathcal{E}\&\mathcal{D}$ ). Table 2 illustrates  $\mathcal{E}\&\mathcal{D}$  achieving the highest performance among three baselines. However, upon integrating multiple teachers from each grain (MT-JG- $\mathcal{E}\&\mathcal{D}$ ), competitive performance is observed compared to the baselines on both FormNLU printed (*P*) (from LiLT 96.5% to 97.21%) and handwritten set (*H*) (from LiLT 97.39% to 97.75%). Still, additional techniques may be necessary to distil the cross-grained multi-teacher information better.

To thoroughly distil joint-grained knowledge from multiple teachers, we introduced multiple loss functions encompassing **Multiple auxiliary tasks**. These functions capture teacher knowledge from inter-grained and cross-grained perspectives, generating representative token embeddings. Typically, using either inter-grained or coarse-grained loss

<sup>4</sup>We chose LLMv3 and LXMERT for JG and select LLMv3&LiLT and VBERT&LXMERT for MT-JG- $\mathcal{E}\&\mathcal{D}$ . More teacher combinations analysis is in Section 5.2.

FG Teacher	CG Teacher	FUNSD	FormNLU	
			<i>P</i>	<i>H</i>
LLmv3	VBERT	90.19	94.72	96.99
	LXMERT	<b>90.57</b>	95.93	<u>97.62</u>
	Transformer	90.22	93.65	95.94
LiLT	VBERT	87.66	<b>97.65</b>	90.53
	LXMERT	87.34	96.76	91.18
	Transformer	87.91	97.20	90.58
LLmv3	VBERT&LXMERT	90.42	95.05	97.25
LLmv3 & LiLT	LXMERT	90.39	96.73	97.42
<b>LLmv3&amp;LiLT</b>	<b>VBERT&amp;LXMERT</b>	<u>90.53</u>	<u>97.21</u>	<b>97.75</b>

Table 3: Comparison of Performance across Teacher Combinations. FG: Fine-Grained, CG: Coarse-Grained, LLMv3: LayoutLMv3, VBERT: VisualBERT. The best is in **bold**. The second best is underlined. This ablation study is based on only Joint Cross Entropy Loss.

individually leads to better performance than the best baselines across various test sets. Inter-grained Similarity (*Sim*) and Distilling (*Distil*) loss consistently achieve higher F1 scores in nearly all test sets. Moreover, cross-grained *Triplet* and alignment (*Align*) losses outperform the best baseline on the FormNLU (*P*) or (*H*). This highlights the effectiveness of the proposed multi-task learning approach in enhancing token representations by integrating knowledge from joint-grained multi-teachers. Inter-grained loss functions exhibit higher robustness on both datasets, whereas cross-grained loss functions only perform well on FormNLU. This difference may stem from the FUNSD being sourced from multiple origins, whereas FormNLU is a single-source dataset. Coarse-grained loss functions may excel on single-source documents by capturing more prevalent knowledge but might introduce noise when applied to multiple sources. Also, the model demonstrates its most competitive performance by integrating all proposed loss functions (+*Sim+Distil+Triplet+Align*). This highlights how the proposed inter-grained and cross-grained loss functions enhance multi-teacher knowledge distillation in form understanding tasks<sup>5</sup>.

## 5.2 Effect of Multi-Teachers

We analysed various teacher combinations to ensure they provide sufficient knowledge for improving joint-grained representations, as depicted in Table 3. For fine-grained teachers, since BROS underperforms compared to others, we only include the performance of its counterparts. The LayoutLMv3-based joint framework performs better, outperforming LiLT-based by approximately 3% on FUNSD and over 5% on FormNLU (*H*).

<sup>5</sup>More loss combination analysis is in Section 5.3

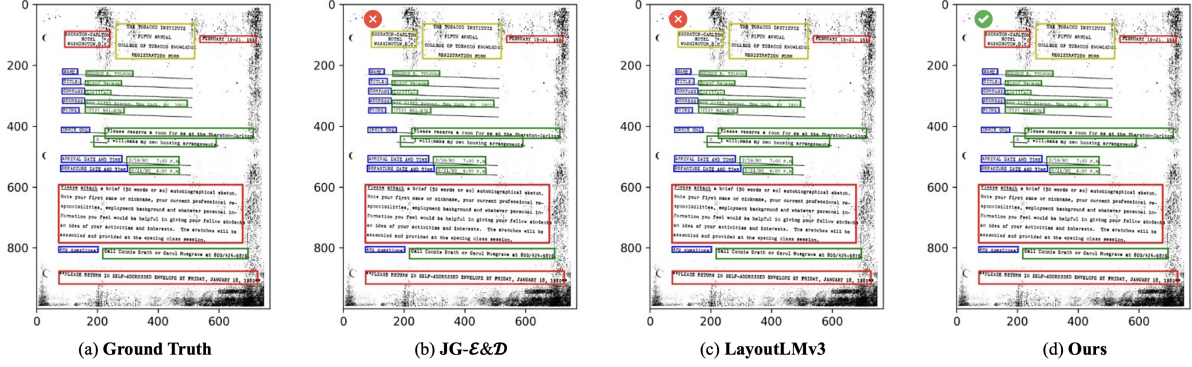


Figure 2: Example output showing (a) Ground Truth (b) JG-E&D (c) LayoutLMv3, and (d) Ours on a FUNSD page. The color code for layout component labels is as follows; Question, Answer, Header, Other. Our model, employing the best loss combination (cross-entropy + similarity) on FUNSD, accurately classified all layout components.

Loss Functions				FUNSD	FormNLU	
Similarity	Distilling	Triplet	Alignment		P	H
O	X	X	X	<b>91.05</b>	98.25	98.09
X	O	X	X	90.90	98.12	97.72
X	X	O	X	90.28	97.58	97.28
X	X	X	O	90.55	97.24	97.42
O	O	X	X	90.63	98.53	97.22
O	X	O	X	90.51	97.71	97.79
O	X	X	O	90.82	97.80	98.05
X	O	O	X	90.82	98.22	<b>98.35</b>
X	O	X	O	90.83	98.63	97.45
O	O	O	X	90.79	98.56	97.72
O	O	X	O	90.66	<b>98.72</b>	97.85
O	O	O	O	<u>90.92</u>	<u>98.69</u>	<b>98.39</b>

Table 4: Performance comparison across loss functions. The best is in **bold**. The second best is underlined.

This improvement can be attributed to the contextual learning facilitated by visual cues. Notably, LiLT achieves the highest performance on the FormNLU ( $P$ ), likely due to its well-designed positional-aware pre-training tasks. For coarse-grained teachers, pre-trained backbones demonstrate better robustness than randomly initialised Transformers, highlighting the benefits of general domain pre-trained knowledge in form understanding tasks. Table 3 illustrates multiple teachers cannot always ensure the best performance, however, the robustness of the proposed model is enhanced by capturing more implicit knowledge from cross-grained teachers.

### 5.3 Effect of Loss Functions

To comprehensively investigate the impact of different loss functions and their combinations, we present the performance of various combinations in Table 4. While employing inter-grained loss individually often proves more effective than using cross-grained loss alone, combining the two losses can enhance knowledge distillation from

joint-grained multi-teachers. For instance, concurrently employing distilling (Distil) and Triplet loss improved accuracy from 97.72% to 98.35%. Notably, stacking all proposed loss functions resulted in the best or second-best performance across all test sets, showcasing their effectiveness in distilling knowledge from multi-teacher to student models for generating more representative representations. Even though cross-grained Triplet and Alignment losses were ineffective individually, when combined with inter-grained loss, they significantly improved knowledge distillation effectiveness.

### 5.4 Qualitative Analysis: Case Studies<sup>6</sup>

We visualised the sample results for the top 3 - Our best model with the best configuration, the best baseline *LayoutLMv3* and the second best baseline *JG-E&D* of FUNSD in Figure 2. We can see that both *LayoutLMv3* and *JG-E&D* have wrongly recognised an *Other* (marked by a white cross in red circle), whereas ours has accurately recognised all document tokens and components.

## 6 Conclusion

We introduced a Multimodal Multi-task Multi-Teacher framework in Visually-Rich form documents. Our model incorporates *multi-teacher*, *multi-task*, and *multi-loss*, and the results show the robustness in capturing implicit knowledge from multi-teachers for understanding diverse form document natures, such as scanned, printed, and handwritten. We hope our work provides valuable insights into leveraging multi-teacher and multi-loss strategies for document understanding research.

<sup>6</sup>A Case Study for FormNLU can be found in Figure 3

## 631 Limitations

632 **Benchmark Scope:** Despite the paramount im-  
633 portance of document understanding across var-  
634 ious domains such as finance, medicine, and re-  
635 sources, our study is constrained by the limited  
636 availability of visually-rich form document under-  
637 standing datasets, particularly those of high quality.  
638 In this research, we solely rely on publicly avail-  
639 able English-based form document understanding  
640 datasets. The scope of benchmark datasets, there-  
641 fore, may not comprehensively represent the di-  
642 versity and complexity present in form documents  
643 across different languages and industries.

644 **Availability of Document Understanding Teach-**  
645 **ers:** The current limitation stems from the reliance  
646 on general document understanding teacher mod-  
647 els due to the absence of large pre-trained form-  
648 specific document models. The availability of high-  
649 quality teachers specifically tailored for form doc-  
650 ument understanding is crucial. Future advance-  
651 ments in the field would benefit from the devel-  
652 opment of dedicated pre-trained models for form  
653 document understanding, providing more accurate  
654 knowledge transfer during training.

## 655 References

656 Srikar Appalaraju, Peng Tang, Qi Dong, Nishant  
657 Sankaran, Yichu Zhou, and R Manmatha. 2023. Doc-  
658 formerv2: Local features for document understand-  
659 ing. *arXiv preprint arXiv:2306.01733*.

660 Yihao Ding, Siqu Long, Jiabin Huang, Kaixuan Ren,  
661 Xingxiang Luo, Hyunsuk Chung, and Soyeon Caren  
662 Han. 2023a. Form-nlu: Dataset for the form natural  
663 language understanding. In *Proceedings of the 46th*  
664 *International ACM SIGIR Conference on Research*  
665 *and Development in Information Retrieval*, pages  
666 2807–2816.

667 Yihao Ding, Siwen Luo, Hyunsuk Chung, and  
668 Soyeon Caren Han. 2023b. Pdf-vqa: A new dataset  
669 for real-world vqa on pdf documents. In *Machine*  
670 *Learning and Knowledge Discovery in Databases:*  
671 *Applied Data Science and Demo Track*, pages 585–  
672 601. Springer Nature Switzerland.

673 Teakgyu Hong, Donghyun Kim, Mingi Ji, Wonseok  
674 Hwang, Daehyun Nam, and Sungrae Park. 2022.  
675 Bros: A pre-trained language model focusing on text  
676 and layout for better key information extraction from  
677 documents. In *Proceedings of the AAAI Conference*  
678 *on Artificial Intelligence*, volume 36, pages 10767–  
679 10775.

680 Yupan Huang, Tengchao Lv, Lei Cui, Yutong Lu, and  
681 Furu Wei. 2022. Layoutlmv3: Pre-training for doc-  
682 ument ai with unified text and image masking. In

*Proceedings of the 30th ACM International Confer-*  
*ence on Multimedia*, pages 4083–4091. 683  
684

Guillaume Jaume, Hazim Kemal Ekenel, and Jean-  
Philippe Thiran. 2019. Funsd: A dataset for form  
understanding in noisy scanned documents. In *2019*  
*International Conference on Document Analysis and*  
*Recognition Workshops (ICDARW)*, volume 2, pages  
1–6. IEEE. 685  
686  
687  
688  
689  
690

Geewook Kim, Teakgyu Hong, Moonbin Yim,  
JeongYeon Nam, Jinyoung Park, Jinyeong Yim, Won-  
seok Hwang, Sangdoon Yun, Dongyoon Han, and Se-  
unghyun Park. 2022. Ocr-free document understand-  
ing transformer. In *Computer Vision–ECCV 2022:*  
*17th European Conference, Tel Aviv, Israel, Octo-*  
*ber 23–27, 2022, Proceedings, Part XXVIII*, pages  
498–517. Springer. 691  
692  
693  
694  
695  
696  
697  
698

Chen-Yu Lee, Chun-Liang Li, Hao Zhang, Timothy  
Dozat, Vincent Perot, Guolong Su, Xiang Zhang,  
Kihyuk Sohn, Nikolay Glushnev, Renshen Wang,  
Joshua Ainslie, Shangbang Long, Siyang Qin, Ya-  
suhisa Fujii, Nan Hua, and Tomas Pfister. 2023a.  
FormNetV2: Multimodal graph contrastive learning  
for form document information extraction. In *Pro-*  
*ceedings of the 61st Annual Meeting of the Associa-*  
*tion for Computational Linguistics (Volume 1: Long*  
*Papers)*, pages 9011–9026. Association for Compu-  
tational Linguistics. 699  
700  
701  
702  
703  
704  
705  
706  
707  
708  
709

Kenton Lee, Mandar Joshi, Iulia Raluca Turc, Hexi-  
ang Hu, Fangyu Liu, Julian Martin Eisenschlos, Ur-  
vashi Khandelwal, Peter Shaw, Ming-Wei Chang, and  
Kristina Toutanova. 2023b. Pix2struct: Screenshot  
parsing as pretraining for visual language understand-  
ing. In *International Conference on Machine Learn-*  
*ing*, pages 18893–18912. PMLR. 710  
711  
712  
713  
714  
715  
716

Liunian Harold Li, Mark Yatskar, Da Yin, Cho-Jui  
Hsieh, and Kai-Wei Chang. 2019. Visualbert: A sim-  
ple and performant baseline for vision and language.  
*arXiv preprint arXiv:1908.03557*. 717  
718  
719  
720

Seunghyun Park, Seung Shin, Bado Lee, Junyeop Lee,  
Jaeheung Surh, Minjoon Seo, and Hwalsuk Lee. 2019.  
Cord: a consolidated receipt dataset for post-ocr  
parsing. In *Workshop on Document Intelligence at*  
*NeurIPS 2019*. 721  
722  
723  
724  
725

Mary Phuong and Christoph Lampert. 2019. Towards  
understanding knowledge distillation. In *Internat-*  
*ional conference on machine learning*, pages 5142–  
5151. PMLR. 726  
727  
728  
729

Yash Srivastava, Vaishnav Murali, Shiv Ram Dubey, and  
Snehasis Mukherjee. 2020. Visual question answer-  
ing using deep learning: A survey and performance  
analysis. In *Computer Vision and Image Processing*  
*- 5th International Conference, CVIP 2020*, volume  
1377 of *Communications in Computer and Informa-*  
*tion Science*, pages 75–86. Springer. 730  
731  
732  
733  
734  
735  
736

Hao Tan and Mohit Bansal. 2019. Lxmert: Learning  
cross-modality encoder representations from trans-  
formers. In *Proceedings of the 2019 Conference on*  
737  
738  
739

- 740 *Empirical Methods in Natural Language Processing*  
741 *and the 9th International Joint Conference on Natu-*  
742 *ral Language Processing (EMNLP-IJCNLP)*, pages  
743 5100–5111.
- 744 Jiapeng Wang, Lianwen Jin, and Kai Ding. 2022. Lilt:  
745 A simple yet effective language-independent layout  
746 transformer for structured document understanding.  
747 In *Proceedings of the 60th Annual Meeting of the*  
748 *Association for Computational Linguistics (Volume*  
749 *1: Long Papers)*, pages 7747–7757.
- 750 Mingliang Zhai, Yulin Li, Xiameng Qin, Chen Yi,  
751 Qunyi Xie, Chengquan Zhang, Kun Yao, Yuwei Wu,  
752 and Yunde Jia. 2023. Fast-structext: An efficient  
753 hourglass transformer with modality-guided dynamic  
754 token merge for document understanding. In *Pro-*  
755 *ceedings of the Thirty-Second International Joint*  
756 *Conference on Artificial Intelligence, IJCAI 2023*,  
757 pages 5269–5277.
- 758 Xu Zhong, Jianbin Tang, and Antonio Jimeno Yepes.  
759 2019. Publaynet: largest dataset ever for document  
760 layout analysis. In *2019 International Conference on*  
761 *Document Analysis and Recognition (ICDAR)*, pages  
762 1015–1022. IEEE.

## A Statistics of tokens and entities

The following Table 5 and 6 demonstrates the number of tokens(length) and number of document entities. While FUNSD has 4 types(Question, Answer, Header, Other) of document entities, FormNLU has 7 types(Title, Section, Form Key, Form Value, Table Key, Table Value, Other). For the FormNLU, we applied two types of test set, including Printed **P** and Handwritten **H**.

FUNSD (Testing)	Question	Answer	Header	Other	Total
Entity	1077	821	122	312	2332
Token	2654	3294	374	2385	8707

Table 5: FUNSD Testing Dataset Distribution by Label.

FormNLU (Testing)	Title	Section	Form Key	Form Value	Table Key	Table Value	Others	Total
<b>P</b> Entity	98	100	346	332	250	249	152	1527
<b>H</b> Entity	100	100	348	315	249	226	149	1487
<b>P</b> Token	700	1258	1934	1557	993	389	3321	10152
<b>H</b> Token	742	1031	1805	866	779	366	2918	8507

Table 6: FormNLU Testing Dataset Distribution by Label, where **P** and **H** are printed and handwritten sets.

## B Breakdown Result Analysis

Model	Config	Overall	Breakdown		
			Header	Question	Answer
LiLT	Teacher	87.54	55.61	90.20	88.34
LayoutLMv3	Teacher	90.61	66.09	91.60	92.78
JG- $\mathcal{E}$	Joint CE	90.45	64.94	91.70	92.67
JG- $\mathcal{D}$	Joint CE	90.48	64.07	91.58	92.73
JG- $\mathcal{E}\&\mathcal{D}$	Joint CE	90.57	64.66	91.48	92.73
MT-JG- $\mathcal{E}\&\mathcal{D}$	Joint CE	90.53	61.24	92.40	91.75
	Sim	91.05	64.81	92.58	92.46
	Distil	90.90	66.96	92.61	91.97
	Triplet	90.28	62.44	92.00	91.44
	Align	90.55	63.81	91.82	92.29
	+Sim+Distil +Triplet+Align	90.92	64.22	92.54	92.31

Table 7: Breakdown Results of FUNSD dataset.

As shown in Table 7, for the FUNSD dataset, we could find all Joint-Grained(JG-) frameworks can have a delicate performance on recognising *Question* and *Answer*, but decreased in Header classification. This might result from the limited number of *Headers* in the FUNSD, leading to inadequate learning of the fine-grained and coarse-grained *Header* information. Multi-task-oriented inter-grained and coarse-grained functions can increase the performance of *Question* recognition by boosting the knowledge distilling from joint-grained multi-teachers. Especially, inter-grained knowledge distillation methods can achieve around 1% higher than LayoutLMv3. The FUNSD dataset

cannot illustrate the benefits of cross-grained loss functions well.

For FormNLU printed and handwritten sets, the joint-grained framework and proposed loss functions can effectively improve *Section (Sec)* and *Title* recognition. As the *Title*, *Section* and *Form\_key (F\_K)* are normally located at similar positions for single-source forms, this may demonstrate both joint-grained framework and multi-task loss function could distil knowledge. Additionally, baseline models are not good at recognising table keys and values, especially handwritten sets. As we use the layoutLMv3 in the joint-grained framework, the performance of recognising table-related tokens is not good for the joint-learning framework. After integrating multiple teachers, the performance has increased from 91.97% to 97.35% on the printed set. The proposed multi-task loss functions may achieve a higher performance of 97.96%. Significant improvements can also be observed across two test sets across all table-related targets. This illustrates that the joint-grained multi-teacher framework can effectively tackle the limitation of one teacher to generate more comprehensive token representations, and the inter-grained and cross-grained loss could boost the effective knowledge exchange to make the generalisation and robustness of the entire framework.

## C Additional Qualitative Analysis

In our qualitative evaluation, we took a closer look at the results by visualising the output of the top two models—our best-performing model with the optimal configuration and the baseline *LayoutLM3*—on the FormNLU handwritten set, as presented in Figure 3. This examination revealed a notable discrepancy between the models. Specifically, *LayoutLM3* exhibited an erroneous identification of the Table Key as a Form Key. In contrast, our model demonstrated a higher level of precision by accurately recognising and distinguishing all components within this intricate and noise-laden handwritten document.

This illustrative case serves as a compelling example highlighting the challenges associated with relying solely on knowledge from a single document to understand teachers. The complexity of distinguishing various document structures, such as the nuanced difference between a form key and a table key, becomes evident. The inadequacy of a singular teacher’s knowledge in capturing such intri-

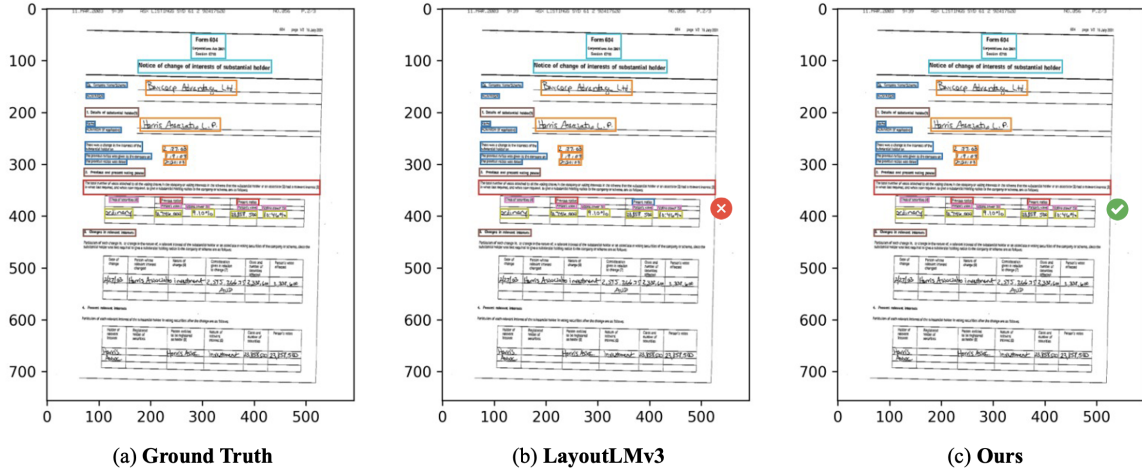


Figure 3: Example output showing (a) Ground Truth (b) LayoutLMv3, and (c) Ours on a FormNLU handwritten test set. The color code for layout component labels is as follows; **Title**, **Section**, **Form Key**, **Form Value**, **Table Key**, **Table Value**, **Other**. Our model, the best loss combination (+Sim+Distil+Triplet+Align) on FormNLU H, accurately classified all layout components.

Model	Config	FormNLU Printed Overall and Breakdown							FormNLU Handwritten Overall and Breakdown						
		Overall	Sec	Title	F_K	F_V	T_K	T_V	Overall	Sec	Title	F_K	F_V	T_K	T_V
LiLT	Teacher	96.50	98.32	96.97	98.84	96.62	96.57	93.60	91.35	95.39	99.50	94.81	90.67	84.19	89.81
LayoutLMv3	Teacher	95.99	98.45	97.96	97.97	96.73	92.37	92.98	97.39	<b>99.33</b>	99.01	<b>99.85</b>	98.24	93.95	95.95
JG- $\mathcal{E}$	Joint CE	94.91	<b>99.66</b>	98.99	98.11	95.73	90.14	90.31	96.55	<b>99.33</b>	99.01	99.42	<b>98.56</b>	88.37	94.67
JG- $\mathcal{D}$	Joint CE	95.68	<b>99.66</b>	<b>100.00</b>	98.55	96.45	91.94	91.10	97.62	<b>99.33</b>	99.01	<b>99.85</b>	<b>98.56</b>	93.02	95.98
JG- $\mathcal{E}\&\mathcal{D}$	Joint CE	95.93	<b>99.66</b>	97.96	97.82	97.18	91.97	92.15	97.62	<b>99.33</b>	99.01	<b>99.85</b>	98.40	93.74	95.75
MT-JG- $\mathcal{E}\&\mathcal{D}$	Joint CE	97.21	99.32	98.48	99.57	96.58	97.35	95.06	97.75	97.67	99.50	99.13	97.93	95.55	96.41
	Sim	98.25	99.32	99.49	99.28	97.75	<b>97.96</b>	<b>97.12</b>	98.09	99.00	<b>100.00</b>	99.27	98.25	<u>96.45</u>	96.61
	Distil	98.12	99.32	<b>100.00</b>	<b>99.71</b>	<b>97.90</b>	<u>97.55</u>	96.30	97.72	97.35	<b>100.00</b>	99.13	97.62	95.75	97.07
	Triplet	97.58	99.32	99.49	99.28	97.18	<u>97.55</u>	95.87	97.28	98.00	<b>100.00</b>	98.83	97.31	93.90	96.83
	Align	97.24	99.32	98.48	<b>99.71</b>	96.57	96.13	95.47	97.42	<b>99.33</b>	99.50	99.13	96.85	92.86	<u>97.52</u>
	+Sim+Distil +Triplet+Align	<b>98.69</b>	99.32	<b>100.00</b>	<b>99.71</b>	<b>99.25</b>	97.35	<b>97.12</b>	<b>98.39</b>	98.33	<b>100.00</b>	99.56	98.09	<b>96.94</b>	<b>97.75</b>

Table 8: Overall and Breakdown Analysis of FormNLU Printed Set and Handwritten Set. The categories of FormNLU dataset Task A include Section (Sec), Title, Form\_Key (F\_K), Form\_Value (F\_V), Table\_Key (T\_K), Table\_Value (T\_V).

837 cacies emphasises the importance of our proposed  
 838 **Multi-modal Multi-task Multi-Teacher** frame-  
 839 work, which leverages insights from multiple teach-  
 840 ers to enhance the robustness and accuracy of form  
 841 document understanding.

## 842 D Additional Implementation Details

843 The table presented in Table 9 outlines the num-  
 844 ber of total parameters and trainable parameters  
 845 across various model configurations. It is evident  
 846 that the choice of teacher models primarily deter-  
 847 mines the total number of parameters. As the num-  
 848 ber of teachers increases, there is a corresponding  
 849 enhancement in the total parameter count. Further-  
 850 more, the architecture of the student model signifi-  
 851 cantly influences the number of trainable parame-  
 852 ters. For instance, encoder-decoder-based student  
 853 models exhibit a higher count of trainable parame-  
 854 ters compared to architectures employing only an

Fine-grained	Coarse-Grained	Configure	# Para	# Trainable
LiLT	N/A	Teacher	130,169,799	130,169,799
LayoutLMv3	N/A	Teacher	125,332,359	125,332,359
	LXMERT	JG-Encoder	393,227,514	19,586,415
		JG-Decoder	423,952,890	50,311,791
	VisualBERT&LXMERT	JG- $\mathcal{E}\&\mathcal{D}$	440,494,842	66,853,743
LXMERT	557,260,798		70,394,991	
Layoutlmv3&LiLT	VisualBERT&LXMERT	LXMERT	574,205,889	68,034,159
		VisualBERT&LXMERT	688,611,013	71,575,407

Table 9: Model configurations and parameters

855 encoder or decoder. This discrepancy implies that  
 856 training encoder-decoder models demands more  
 857 computational resources. Despite the variation  
 858 in trainable parameters among different student  
 859 model architectures, it is noteworthy that the over-  
 860 all number remains substantially smaller than that  
 861 of single-teacher fine-tuning processes. This obser-  
 862 vation underscores the efficiency of student model  
 863 training in comparison to fine-tuning pre-trained  
 864 models.